

# *GES Long Baseline Navigation with Unknown Sound Velocity and Discrete-time Range Measurements*

Pedro Batista

*IEEE Transactions on Control Systems Technology*, vol. 23, no. 1,  
pp. 219-230, January 2015

<https://doi.org/10.1109/TCST.2014.2321973>

© 20XX IEEE. Personal use of this material is permitted. Permission from IEEE must be obtained for all other uses, in any current or future media, including reprinting/republishing this material for advertising or promotional purposes, creating new collective works, for resale or redistribution to servers or lists, or reuse of any copyrighted component of this work in other works.

## Accepted Version

Level of access, as per info available on SHERPA/ROMEO

<http://www.sherpa.ac.uk/romeo/search.php>















IEEE Transactions on Control Systems Technology

### Publication Information

|            |   |
|------------|---|
| Title      | IEEE Transactions on Control Systems Technology [English]   |
| ISSNs      | Print: 1063-6536<br>Electronic: 1558-0865   |
| URL        | <a href="http://ieeexplore.ieee.org/xpl/RecentIssue.jsp?punumber=87">http://ieeexplore.ieee.org/xpl/RecentIssue.jsp?punumber=87</a> |
| Publishers | Institute of Electrical and Electronics Engineers [Society Publisher]   |

### Publisher Policy

Open Access pathways permitted by this journal's policy are listed below by article version. Click on a pathway for a more detailed view.

|   |  |   |
|---|--|---|
| Published Version   |  None   | + |
|   | <a href="#">Journal Website</a>  |   |
| Accepted Version<br>[pathway a]   | None    | - |
|   | <a href="#">Any Repository</a> , <a href="#">arXiv</a> , <a href="#">Institutional Website</a> , +3  |   |
|  Embargo         | No Embargo   |   |
|  Copyright Owner | Publishers   |   |
|  Location        | Any Repository<br>Author's Homepage<br>Institutional Repository<br>Institutional Website<br>Named Repository (arXiv, TechRxiv)   |   |
|  Conditions      | When accepted for publication, set statement to accompany deposit (see policy)<br>Must link to publisher version with DOI<br>Publisher copyright and source must be acknowledged   |   |
| Accepted Version<br>[pathway b]   |  24m    | + |
|   | <a href="#">arXiv</a> , <a href="#">Funder Designated Location</a> , <a href="#">Institutional Website</a>   |   |
| Submitted Version<br>[pathway a]  | None    | + |
|   | <a href="#">arXiv</a> , <a href="#">Funder Designated Location</a> , <a href="#">TechRxiv</a> , +3   |   |
| Submitted Version<br>[pathway b]  | None     | + |
|   | <a href="#">Academic Social Network</a>  |   |

For more information, please see the following links:

- IEEE Copyright Policy
- Section 8.1.9 of the PSPB Operations Manual
- Policy: Posting Your Article
- IEEE Open
- Author Posting of IEEE Copyrighted Papers Online
- Electronic IEEE Copyright Form

# GES Long Baseline Navigation with Unknown Sound Velocity and Discrete-time Range Measurements

Pedro Batista, *Member, IEEE*

**Abstract**—A common assumption in long baseline (LBL) underwater acoustic navigation is that the speed of sound is available. This quantity depends on the medium and it is usually measured or profiled prior to the experiments. This paper proposes a novel filtering solution that explicitly takes into account the estimation of the speed of propagation of the acoustic waves in the medium. Based on discrete-time range measurements, an augmented system is derived that can be regarded as linear for observability and observer design purposes. Its observability is discussed and a Kalman filter provides the estimation solution, with globally exponentially stable (GES) error dynamics. Simulation results are presented, considering noisy measurements, to evaluate the proposed solution, which evidences both fast convergence and good performance.

## I. INTRODUCTION

LONG baseline (LBL) navigation is a common solution for positioning of underwater vehicles, resorting in general to the round-trip travel time of acoustic signals from the vehicle to several transponders, fixed in known positions in the mission scenario. In [1] a LBL underwater acoustic localization system that was developed to provide three-dimensional position information for the Seaglider underwater vehicle is discussed. The positioning system relies on acoustic round-trip travel time measurements that are processed by an extended Kalman filter (EKF). If data are available for post-processing, further improvements were achieved by using a Rauch-Tung-Striebel smoother. The performance of the system was assessed both in simulation and with experiments. In [2] the authors consider a Doppler Velocity Log (DVL) and compare the performance of a combined LBL/DVL solution, consisting of a complementary filter navigation system, with that of standalone Doppler of LBL navigation. In [3] two different approaches are compared for long baseline navigation. In the first, so-called fix-computation method, dead-reckoning from the last acoustic fix is performed and a reset occurs whenever a new fix is available. In the second, so-called filtering approach, an EKF is employed and, whenever a valid travel-time is available, the filter updates the state estimates. In [4] a review of underwater vehicle navigation is offered and preliminary field trials of DVLNAV, an interactive program for 3-D navigation of underwater vehicles, are reported. In [5] the concept of long baselines navigation is extended to the case where measurements to a single acoustic source are available, by combining dead-reckoning and rich trajectories to ensure so-called Synthetic Long Baseline. Alternative solutions with single range measurements can be found in [6] and [7], where

EKFs have been extensively used to solve the navigation problem based on single beacon range measurements. In [8] the study of observability of single transponder underwater navigation was carried out resorting to an algebraic approach and algebraic observers were also proposed. In [9] preliminary experimental results with single beacon acoustic navigation were presented, where the EKF is employed as the state estimator. In [10] the author proposes a GPS-like system consisting of buoys equipped with Differential GPS. A related solution, denominated as GPS Intelligent Buoy (GIB) system, is now commercially available, see [11]. Further work on the GIB underwater positioning system can be found in [12]. For interesting discussions and detailed surveys on underwater vehicle navigation techniques and challenges see [13], [14], and [15].

In previous work by the authors a novel filtering solution was proposed for long baseline navigation [16], based on an extension of the framework for single range measurements, proposed in [17], to multiple range measurements. A common assumption, present in all previously mentioned contributions, is that the speed of propagation of the waves in the medium is known or measured. This quantity depends on several characteristics such as the salinity, pressure, and temperature and it is either measured or profiled, often prior to the experiments. If that is not the case, or even for small errors of the sound velocity profile, the range measurements can carry large errors, particularly when the distances become large, thus putting into question the entire navigation data. The main contribution of this paper is the development of a novel framework for long baseline navigation that explicitly includes the estimation of the speed of propagation of the acoustic waves in the medium. Based on discrete-time range measurements, combined with attitude and relative velocity readings obtained at high rates, an augmented system is derived that can be considered as linear for observability and observer design purposes. Its observability is carefully analyzed and a Kalman filter is considered as the estimation solution, with globally exponentially stable error dynamics. Previous work can be found in [18]. This paper provides detailed results and proofs and extensive simulation results, including comparison with the EKF and Monte Carlo simulations.

The paper is organized as follows. The problem statement and the nominal system dynamics are introduced in Section II, while the filter design is detailed in Section III. Simulation results are presented in Section IV and Section V summarizes the main results of the paper.

### A. Notation

Throughout the paper the symbol  $\mathbf{0}$  denotes a matrix of zeros and  $\mathbf{I}$  an identity matrix, both of appropriate dimensions.

This work was supported by the FCT [PEst-OE/EEI/LA0009/2013].

The author is with the Institute for Systems and Robotics, Instituto Superior Técnico, Universidade de Lisboa, Av. Rovisco Pais, 1049-001 Lisboa, Portugal. Email: pbatista@isr.ist.utl.pt

A block diagonal matrix is represented by  $\text{diag}(\mathbf{A}_1, \dots, \mathbf{A}_n)$ . For  $\mathbf{x} \in \mathbb{R}^3$  and  $\mathbf{y} \in \mathbb{R}^3$ ,  $\mathbf{x} \cdot \mathbf{y}$  represents the inner product.

## II. PROBLEM STATEMENT

Consider a standard Long Baseline acoustic positioning system, consisting of a set of transponders that are fixed in the mission scenario, where an underwater vehicle operates, also equipped with an acoustic transponder, as depicted in Fig. 1. Typically, the transponder of the vehicle sends a known

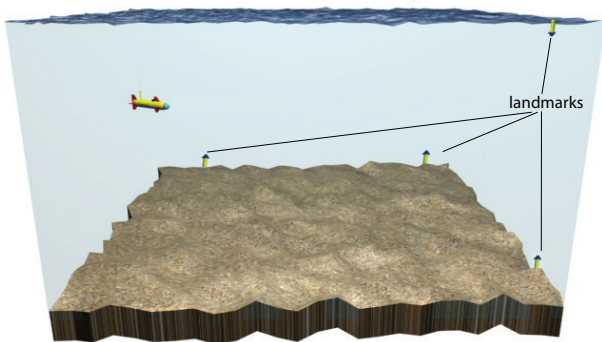


Fig. 1. Long baseline mission scenario

acoustic signal to interrogate the transponders of the Long Baseline acoustic positioning system, which then respond sending each a known acoustic signal. These signals are then received by the transponder of the vehicle and the range is usually calculated using the round-trip travel time and the speed of propagation of the acoustic waves in the medium. In this paper, the latter is assumed unknown and as such the range measurements, which are measured periodically, are only available up to a scaling factor. Further suppose that the vehicle is equipped with an Attitude and Heading Reference System (AHRS) and a DVL. The problem considered herein is that of designing a continuous-discrete filter, with globally exponentially stable error dynamics, to estimate the position and linear velocity of the vehicle, as well as the speed of propagation of the acoustic waves in the medium.

### A. System dynamics

Let  $\{I\}$  denote a local inertial reference coordinate frame and  $\{B\}$  a coordinate frame attached to the vehicle, usually referred to as the body-fixed reference frame. The linear motion of the vehicle satisfies

$$\dot{\mathbf{p}}(t) = \mathbf{R}(t)\mathbf{v}(t), \quad (1)$$

where  $\mathbf{p}(t) \in \mathbb{R}^3$  denotes the inertial position of the vehicle,  $\mathbf{v}(t) \in \mathbb{R}^3$  is the velocity of the vehicle relative to  $\{I\}$ , expressed in body-fixed coordinates, and  $\mathbf{R}(t) \in SO(3)$  is the rotation matrix from  $\{B\}$  to  $\{I\}$ .

The AHRS provides the rotation matrix  $\mathbf{R}(t)$ , while the DVL measures, in the absence of bottom-lock, the velocity of the vehicle relative to the fluid, expressed in body-fixed coordinates. Let  $\mathbf{v}_c(t) \in \mathbb{R}^3$  denote the velocity of the fluid, in inertial coordinates, and  $\mathbf{v}_r(t) \in \mathbb{R}^3$  be the DVL reading,

i.e., the velocity of the vehicle relative to the fluid, expressed in body-fixed coordinates. Then,

$$\mathbf{v}(t) = \mathbf{v}_r(t) + \mathbf{R}^T(t)\mathbf{v}_c(t). \quad (2)$$

Finally, let  $\mathbf{s}_i \in \mathbb{R}^3$ ,  $i = 1, \dots, L$ , denote the inertial positions of the transponders. Then, the range measurements are given by

$$r_i(k) = v_s(t) \|\mathbf{s}_i - \mathbf{p}(t_k)\|, \quad i = 1, \dots, L, \quad (3)$$

with  $t_k := t_0 + kT$ ,  $k \in \mathbb{N}$ , where  $T > 0$  is the sampling period,  $t_0$  is the initial time, and  $v_s(t) > 0$  is a dimensionless scaling factor that accounts for the unknown speed of propagation of the acoustic waves in the medium. In short, a nominal speed of propagation is assumed by the range sensor, which does not necessarily correspond to the actual speed of propagation, which is assumed unknown. The scaling factor  $v_s(t)$  accounts for that relation.

Assuming that both the fluid velocity and the speed of propagation of the acoustic waves in the medium are constant, i.e.,  $\dot{\mathbf{v}}_c(t) = \mathbf{0}$  and  $\dot{v}_s(t) = 0$ , and combining (1)-(3), results in the nonlinear system with discrete outputs

$$\begin{cases} \dot{\mathbf{p}}(t) = \mathbf{v}_c(t) + \mathbf{R}(t)\mathbf{v}_r(t) \\ \dot{\mathbf{v}}_c(t) = \mathbf{0} \\ \dot{v}_s(t) = 0 \\ r_1(k) = v_s(t_k) \|\mathbf{s}_1 - \mathbf{p}(t_k)\| \\ \vdots \\ r_L(k) = v_s(t_k) \|\mathbf{s}_L - \mathbf{p}(t_k)\| \end{cases} \cdot \quad (4)$$

The problem considered herein is the design of an estimator for (4) with globally exponentially stable error dynamics.

## III. FILTER DESIGN

In previous work by the authors [16] a novel LBL framework was proposed in continuous time. In short, additional states and outputs are derived that allow one to consider the system as linear in the state, even though it still is, in fact, nonlinear. This is done by means of identification of some nonlinear terms as new variables and noticing that the output and input are available signals for observer design purposes. In this paper, a similar approach is somehow pursued, in the sense that state and output augmentation are performed, but considering: i) discrete-time measurements; and ii) scaled ranges, with unknown speed of propagation of the acoustic waves in the medium. This setting leads to a different state vector and consequently a different dynamic system, and captures the nature of the underwater ranging sensing system when the speed of propagation is unknown or only known approximately.

### A. Discretization and system augmentation

The exact discrete-time system dynamics corresponding to (4) are given by

$$\begin{cases} \mathbf{p}(t_{k+1}) = \mathbf{p}(t_k) + T\mathbf{v}_c(t_k) + \int_{t_k}^{t_{k+1}} \mathbf{R}(\tau) \mathbf{v}_r(\tau) d\tau \\ \mathbf{v}_c(t_{k+1}) = \mathbf{v}_c(t_k) \\ v_s(t_{k+1}) = v_s(t_k) \\ r_1(k) = v_s(t_k) \|\mathbf{s}_1 - \mathbf{p}(t_k)\| \\ \vdots \\ r_L(k) = v_s(t_k) \|\mathbf{s}_L - \mathbf{p}(t_k)\| \end{cases} \quad (5)$$

Define the discrete-time states

$$\begin{cases} \mathbf{x}_1(k) := v_s^2(t_k) \mathbf{p}(t_k) \\ \mathbf{x}_2(k) := v_s^2(t_k) \mathbf{v}_c(t_k) \\ x_3(k) = v_s^2(t_k) \end{cases} \quad .$$

From (5) one may write

$$\begin{cases} \mathbf{x}_1(k+1) = \mathbf{x}_1(k) + T\mathbf{x}_2(k) + x_3(k) \mathbf{u}(k) \\ \mathbf{x}_2(k+1) = \mathbf{x}_2(k) \\ x_3(k+1) = x_3(k) \end{cases} \quad , \quad (6)$$

where

$$\mathbf{u}(k) := \int_{t_k}^{t_{k+1}} \mathbf{R}(\tau) \mathbf{v}_r(\tau) d\tau.$$

Now, consider the scaled range measurements as additional system states, i.e., define

$$\begin{cases} x_4(k) := r_1(k) \\ \vdots \\ x_{3+L}(k) := r_L(k) \end{cases} \quad .$$

To derive the discrete-time dynamics of the range measurements, consider their squares and expand

$$r_i^2(k+1) = x_3(k+1) \left\| \mathbf{s}_i - \frac{\mathbf{x}_1(k+1)}{x_3(k+1)} \right\|^2$$

using (6), which gives

$$\begin{aligned} r_i^2(k+1) &= r_i^2(k) + 2\mathbf{u}(k) \cdot \mathbf{x}_1(k) \\ &\quad - 2T[\mathbf{s}_i - \mathbf{u}(k)] \cdot \mathbf{x}_2(k) \\ &\quad - [2\mathbf{s}_i - \mathbf{u}(k)] \cdot \mathbf{u}(k) x_3(k) \\ &\quad + 2T \frac{\mathbf{x}_1(k) \cdot \mathbf{x}_2(k)}{x_3(k)} \\ &\quad + T^2 \frac{\|\mathbf{x}_2(k)\|^2}{x_3(k)}, \end{aligned} \quad (7)$$

$i = 1, \dots, L$ . Identifying the nonlinear terms  $\mathbf{x}_1(k) \cdot \mathbf{x}_2(k)/x_3(k)$  and  $\|\mathbf{x}_2(k)\|^2/x_3(k)$  in (7) with new system states, i.e.,

$$\begin{cases} x_{4+L}(k) := \frac{\mathbf{x}_1(k) \cdot \mathbf{x}_2(k)}{x_3(k)} = v_s^2(t_k) \mathbf{p}(t_k) \cdot \mathbf{v}_c(t_k) \\ x_{5+L}(k) := \frac{\|\mathbf{x}_2(k)\|^2}{x_3(k)} = v_s^2(t_k) \|\mathbf{v}_c(t_k)\|^2 \end{cases} \quad , \quad (8)$$

and noticing that  $r_i^2(k) = x_{3+i}(k)r_i(k)$ ,  $i = 1, \dots, L$ , allows one to write

$$\begin{aligned} x_{3+i}(k+1) &= \frac{2\mathbf{u}(k) \cdot \mathbf{x}_1(k)}{r_i(k+1)} - \frac{2T[\mathbf{s}_i - \mathbf{u}(k)] \cdot \mathbf{x}_2(k)}{r_i(k+1)} \\ &\quad - \frac{[2\mathbf{s}_i - \mathbf{u}(k)] \cdot \mathbf{u}(k)}{r_i(k+1)} x_3(k) \\ &\quad + \frac{r_i(k) x_{3+i}(k)}{r_i(k+1)} + \frac{2Tx_{4+L}(k)}{r_i(k+1)} \\ &\quad + \frac{T^2 x_{5+L}(k)}{r_i(k+1)}, \end{aligned}$$

$i = 1, \dots, L$ . The evolution of the new states can be written, using (6), as

$$\begin{cases} x_{4+L}(k+1) = \mathbf{u}(k) \cdot \mathbf{x}_2(k) + x_{4+L}(k) + Tx_{5+L}(k) \\ x_{5+L}(k+1) = x_{5+L}(k) \end{cases} \quad .$$

Define the augmented state vector as

$$\mathbf{x}(k) := \begin{bmatrix} \mathbf{x}_1(k) \\ \mathbf{x}_2(k) \\ x_3(k) \\ x_4(k) \\ \vdots \\ x_{3+L}(k) \\ x_{4+L}(k) \\ x_{5+L}(k) \end{bmatrix} \in \mathbb{R}^{3+3+1+L+2}.$$

Then, the discrete-time system dynamics can be written as

$$\mathbf{x}(k+1) = \mathbf{A}(k) \mathbf{x}(k),$$

where  $\mathbf{A}(k) \in \mathbb{R}^{(7+L+2) \times (7+L+2)}$ ,

$$\mathbf{A}(k) = \begin{bmatrix} \mathbf{I} & T\mathbf{I} & \mathbf{u}(k) & \mathbf{0} & \mathbf{0} & \mathbf{0} & \mathbf{0} \\ \mathbf{0} & \mathbf{I} & \mathbf{0} & \mathbf{0} & \mathbf{0} & \mathbf{0} & \mathbf{0} \\ \mathbf{0} & \mathbf{0} & 1 & \mathbf{0} & \mathbf{0} & \mathbf{0} & \mathbf{0} \\ \mathbf{A}_{21}(k) & \mathbf{A}_{22}(k) & \vdots & \vdots & \vdots & \vdots & \vdots \\ \mathbf{0} & \mathbf{u}^T(k) & 0 & \mathbf{0} & 1 & T \\ \mathbf{0} & \mathbf{0} & 0 & \mathbf{0} & 0 & 1 \end{bmatrix},$$

with  $\mathbf{A}_{21}(k) \in \mathbb{R}^{L \times 7}$

$$\mathbf{A}_{21}(k) = \begin{bmatrix} \frac{2\mathbf{u}^T(k)}{r_1(k+1)} & 2T \frac{\mathbf{u}^T(k) - \mathbf{s}_1^T}{r_1(k+1)} & \frac{\mathbf{u}(k) - 2\mathbf{s}_1}{r_1(k+1)} \cdot \mathbf{u}(k) \\ \vdots & \vdots & \vdots \\ \frac{2\mathbf{u}^T(k)}{r_L(k+1)} & 2T \frac{\mathbf{u}^T(k) - \mathbf{s}_L^T}{r_L(k+1)} & \frac{\mathbf{u}(k) - 2\mathbf{s}_L}{r_L(k+1)} \cdot \mathbf{u}(k) \end{bmatrix},$$

and

$$\mathbf{A}_{22}(k) = \text{diag} \left( \frac{r_1(k)}{r_1(k+1)}, \dots, \frac{r_L(k)}{r_L(k+1)} \right) \in \mathbb{R}^{L \times L}.$$

To encode the LBL structure in the system dynamics, i.e., to include the geometry of the LBL array in the system dynamics, take the difference of the squares of range measurements to two different transponders, which gives

$$\begin{aligned} r_i^2(t_k) - r_j^2(t_k) &= v_s^2(t_k) \left( \|\mathbf{s}_i\|^2 - \|\mathbf{s}_j\|^2 \right) \\ &\quad - 2v_s^2(t_k) [(\mathbf{s}_i - \mathbf{s}_j) \cdot \mathbf{p}(t_k)]. \end{aligned} \quad (9)$$

Using

$$r_i^2(k) - r_j^2(k) = [r_i(k) + r_j(k)] [x_{3+i}(k) - x_{3+j}(k)]$$

allows one to rewrite (9) as

$$\frac{2(\mathbf{s}_i - \mathbf{s}_j)}{r_i(k) + r_j(k)} \cdot \mathbf{x}_1(k) - \frac{\|\mathbf{s}_i\|^2 - \|\mathbf{s}_j\|^2}{r_i(k) + r_j(k)} x_3(k) + x_{3+i}(k) - x_{3+j}(k) = 0 \quad (10)$$

for  $i, j \in \{1, \dots, L\}$ ,  $i \neq j$ . Discarding the original nonlinear output equation, considering that the states  $x_4(k), \dots, x_{3+L}(k)$  are measured, and using (10) allows one to define the augmented system output

$$\begin{cases} y_1(k) = x_4(k) \\ \vdots \\ y_L(k) = x_{3+L}(k) \\ y_{L+1}(k) = \frac{2(\mathbf{s}_1 - \mathbf{s}_2) \cdot \mathbf{x}_1(k)}{r_1(k) + r_2(k)} - \frac{\|\mathbf{s}_1\|^2 - \|\mathbf{s}_2\|^2}{r_1(k) + r_2(k)} x_3(k) \\ \quad + x_{3+1}(k) - x_{3+2}(k) \\ y_{L+2}(k) = \frac{2(\mathbf{s}_1 - \mathbf{s}_3) \cdot \mathbf{x}_1(k)}{r_1(k) + r_3(k)} - \frac{\|\mathbf{s}_1\|^2 - \|\mathbf{s}_3\|^2}{r_1(k) + r_3(k)} x_3(k) \\ \quad + x_{3+1}(k) - x_{3+3}(k) \\ \vdots \\ y_{L+C_2^{L-1}}(k) = \frac{2(\mathbf{s}_{L-2} - \mathbf{s}_L) \cdot \mathbf{x}_1(k)}{r_{L-2}(k) + r_L(k)} - \frac{\|\mathbf{s}_{L-2}\|^2 - \|\mathbf{s}_L\|^2}{r_{L-2}(k) + r_L(k)} x_3(k) \\ \quad + x_{3+L-2}(k) - x_{3+L}(k) \\ y_{L+C_2^L}(k) = \frac{2(\mathbf{s}_{L-1} - \mathbf{s}_L) \cdot \mathbf{x}_1(k)}{r_{L-1}(k) + r_L(k)} - \frac{\|\mathbf{s}_{L-1}\|^2 - \|\mathbf{s}_L\|^2}{r_{L-1}(k) + r_L(k)} x_3(k) \\ \quad + x_{3+L-1}(k) - x_{3+L}(k) \end{cases},$$

where  $C_2^L$  is the number of 2-combinations of  $L$  elements, i.e.  $C_2^L = L(L-1)/2$ .

The discrete-time augmented system can then be written, in compact form, as

$$\begin{cases} \mathbf{x}(k+1) = \mathbf{A}(k) \mathbf{x}(k) \\ \mathbf{y}(k+1) = \mathbf{C}(k+1) \mathbf{x}(k+1) \end{cases}, \quad (11)$$

with

$$\mathbf{C}(k) = \begin{bmatrix} \mathbf{0} & \mathbf{I} & \mathbf{0} \\ \mathbf{C}_{21}(k) & \mathbf{C}_{22} & \mathbf{0} \end{bmatrix} \in \mathbb{R}^{(L+C_2^L) \times (7+L+2)},$$

where  $\mathbf{C}_{21}(k) \in \mathbb{R}^{C_2^L \times 7}$  is given by

$$\mathbf{C}_{21}(k) = \begin{bmatrix} \frac{2(\mathbf{s}_1 - \mathbf{s}_2)^T}{r_1(k) + r_2(k)} & \mathbf{0} & -\frac{\|\mathbf{s}_1\|^2 - \|\mathbf{s}_2\|^2}{r_1(k) + r_2(k)} \\ \frac{2(\mathbf{s}_1 - \mathbf{s}_3)^T}{r_1(k) + r_3(k)} & \mathbf{0} & -\frac{\|\mathbf{s}_1\|^2 - \|\mathbf{s}_3\|^2}{r_1(k) + r_3(k)} \\ \vdots & \vdots & \vdots \\ \frac{2(\mathbf{s}_{L-2} - \mathbf{s}_L)^T}{r_{L-2}(k) + r_L(k)} & \mathbf{0} & -\frac{\|\mathbf{s}_{L-2}\|^2 - \|\mathbf{s}_L\|^2}{r_{L-2}(k) + r_L(k)} \\ \frac{2(\mathbf{s}_{L-1} - \mathbf{s}_L)^T}{r_{L-1}(k) + r_L(k)} & \mathbf{0} & -\frac{\|\mathbf{s}_{L-1}\|^2 - \|\mathbf{s}_L\|^2}{r_{L-1}(k) + r_L(k)} \end{bmatrix},$$

and

$$\mathbf{C}_{22} = \begin{bmatrix} 1 & -1 & 0 & \dots & \dots & \dots & 0 \\ 1 & 0 & -1 & 0 & \dots & \dots & 0 \\ & & \vdots & & & & \\ 0 & \dots & \dots & 0 & 1 & 0 & -1 \\ 0 & \dots & \dots & \dots & 0 & 1 & -1 \end{bmatrix} \in \mathbb{R}^{C_2^L \times L}.$$

*Remark 1:* Notice that the system (11) is well defined as no range measurement can be nonpositive. Indeed, by definition, the range measurements are nonnegative and a null measurement would imply that two transponders were in the same position, which is impossible. In fact, there is always a minimum distance between transponders.

## B. Observability analysis

The system (11) can be regarded as a discrete linear time-varying system for observer design purposes, even though the system matrices  $\mathbf{A}(k)$  and  $\mathbf{C}(k)$  depend on the system input and the range measurements. This is possible because for observer (or filter) design purposes both the ranges and the input are available and, hence, they can be simply considered as functions of time. This idea was first pursued by the authors in [17, Lemma 1] for continuous systems, whose application is equivalent for the discrete-time case, as shown in the following lemma.

*Lemma 1:* Consider the nonlinear discrete-time system

$$\begin{cases} \mathbf{x}(k+1) = \mathbf{A}(k, \mathbf{u}_{k_0}^{k+1}, \mathbf{y}_{k_0}^{k+1}) \mathbf{x}(k) \\ \mathbf{y}(k+1) = \mathbf{C}(k+1, \mathbf{u}_{k_0}^{k+1}, \mathbf{y}_{k_0}^{k+1}) \mathbf{x}(k+1) \end{cases}, \quad (12)$$

where  $\mathbf{u}_{k_0}^{k_f} := \{\mathbf{u}(k_0), \mathbf{u}(k_0+1), \dots, \mathbf{u}(k_f)\}$  and  $\mathbf{y}_{k_0}^{k_f} := \{\mathbf{y}(k_0), \mathbf{y}(k_0+1), \dots, \mathbf{y}(k_f)\}$  are the input and output signals, respectively, on the time interval  $[k_0, k_f]$ , and  $\mathbf{x}(k) \in \mathbb{R}^n$ . If  $\text{rank}(\mathcal{O}(k_0, k_f)) = n$ , where  $\mathcal{O}(k_0, k_f)$  is the observability matrix associated with the pair  $(\mathbf{A}(k, \mathbf{u}_{k_0}^{k_f-1}, \mathbf{y}_{k_0}^{k_f-1}), \mathbf{C}(k, \mathbf{u}_{k_0}^{k_f-1}, \mathbf{y}_{k_0}^{k_f-1}))$  on  $\mathcal{I} := [k_0, k_f]$ , then the nonlinear system (12) is observable on  $\mathcal{I}$  in the sense that, given the system input and output signals  $\mathbf{u}_{k_0}^{k_f-1}$  and  $\mathbf{y}_{k_0}^{k_f-1}$ , the initial condition  $\mathbf{x}(k_0)$  is uniquely defined.

*Proof:* For the sake of ease of notation, and as both the system input and output signals  $\mathbf{u}_{k_0}^{k_f-1}$  and  $\mathbf{y}_{k_0}^{k_f-1}$  are assumed available, consider the simplified notation  $\mathbf{A}(k) = \mathbf{A}(k, \mathbf{u}_{k_0}^{k+1}, \mathbf{y}_{k_0}^{k+1})$  and  $\mathbf{C}(k+1) = \mathbf{C}(k+1, \mathbf{u}_{k_0}^{k+1}, \mathbf{y}_{k_0}^{k+1})$ . Given  $\mathbf{u}_{k_0}^{k_f}$  and  $\mathbf{y}_{k_0}^{k_f}$ , it is possible to compute the transition matrix associated with the system matrix  $\mathbf{A}(k)$ , given by  $\phi(k, k_0) = \mathbf{A}(k-1) \mathbf{A}(k-2) \dots \mathbf{A}(k_0)$  for  $k_0 < k \leq k_f$ , with  $\phi(k_0, k_0) = \mathbf{I}$ . Hence, it is possible to compute the observability matrix

$$\mathcal{O}(k_0, k_f) = \begin{bmatrix} \mathbf{C}(k_0) \\ \mathbf{C}(k_0+1) \phi(k_0+1, k_0) \\ \vdots \\ \mathbf{C}(k_f-1) \phi(k_f-1, k_0) \end{bmatrix}.$$

Now, notice that it is possible to write the evolution of the state, given the system input and output (which allow one to compute the transition matrix), as

$$\mathbf{x}(k) = \phi(k, k_0) \mathbf{x}_0 \quad (13)$$

for  $k_0 < k < k_f$ , where  $\mathbf{x}_0 = \mathbf{x}(k_0)$  is the initial condition. This is easily verified by substitution into the state equation. The remainder of the proof follows as in classic theory. The output of the system can be written, from (13), as

$$\mathbf{y}(k) = \mathbf{C}(k) \phi(k, k_0) \mathbf{x}_0$$

for  $k_0 < k < k_f$ , with  $\mathbf{y}(k_0) = \mathbf{C}(k_0) \mathbf{x}_0$ . Considering the output for all available time instants gives

$$\begin{bmatrix} \mathbf{y}(k_0) \\ \mathbf{y}(k_0+1) \\ \mathbf{y}(k_0+2) \\ \vdots \\ \mathbf{y}(k_f-1) \end{bmatrix} = \mathcal{O}(k_0, k_f) \mathbf{x}_0. \quad (14)$$

Multiplying (14) on both sides by  $\mathcal{O}^T(k_0, k_f)$  yields

$$\mathcal{W}(k_0, k_f) \mathbf{x}_0 = \mathcal{O}^T(k_0, k_f) \begin{bmatrix} \mathbf{y}(k_0) \\ \mathbf{y}(k_0 + 1) \\ \mathbf{y}(k_0 + 2) \\ \vdots \\ \mathbf{y}(k_f - 1) \end{bmatrix}, \quad (15)$$

where  $\mathcal{W}(k_0, k_f) := \mathcal{O}^T(k_0, k_f) \mathcal{O}(k_0, k_f)$  is the observability Gramian associated with the pair  $(\mathcal{A}(k), \mathcal{C}(k))$  on  $\mathcal{I}$ . All quantities in (15) but  $\mathbf{x}_0$  are known given the system input and output and as such (15) is a linear algebraic equation on  $\mathbf{x}_0$ . Hence, if  $\text{rank}(\mathcal{O}(k_0, k_f)) = n$ , the observability Gramian  $\mathcal{W}(k_0, k_f)$  is invertible and therefore  $\mathbf{x}_0$  is uniquely defined, concluding the proof. ■

*Remark 2:* It is important to stress that, even though (13) resembles, at first glance, the zero-input response of a linear system, that is not the case because the transition matrix in (13) depends explicitly on the system input and output. Moreover, the superposition principle does not necessarily apply. However, that is not a problem for observability and observer design purposes as both the input and output signals are assumed available.

The following result addresses the observability of the nonlinear discrete-time system (11).

*Theorem 1:* Suppose that the configuration of the Long Baseline acoustic positioning system is such that

$$\mathbf{L} := \begin{bmatrix} 2(\mathbf{s}_1 - \mathbf{s}_2)^T & -\left(\|\mathbf{s}_1\|^2 - \|\mathbf{s}_2\|^2\right) \\ 2(\mathbf{s}_1 - \mathbf{s}_3)^T & -\left(\|\mathbf{s}_1\|^2 - \|\mathbf{s}_3\|^2\right) \\ \vdots & \vdots \\ 2(\mathbf{s}_{L-2} - \mathbf{s}_L)^T & -\left(\|\mathbf{s}_{L-2}\|^2 - \|\mathbf{s}_L\|^2\right) \\ 2(\mathbf{s}_{L-1} - \mathbf{s}_L)^T & -\left(\|\mathbf{s}_{L-1}\|^2 - \|\mathbf{s}_L\|^2\right) \end{bmatrix} \in \mathbb{R}^{C_L^2 \times 4}$$

is full rank, i.e.,

$$\text{rank}(\mathbf{L}) = 4. \quad (16)$$

Then, the discrete-time system (11) is observable on any interval  $[k_i, k_{i+3}]$ ,  $k_i = 0, 1, 2, \dots$ , in the sense that the initial state  $\mathbf{x}(k_i)$  is uniquely determined by the input  $\{\mathbf{u}(k) : k = k_i, k_{i+1}, k_{i+2}\}$  and the output  $\{\mathbf{y}(k) : k = k_i, k_{i+1}, k_{i+2}\}$ .

*Proof:* The proof resorts to Lemma 1 and it reduces to show that the observability matrix  $\mathcal{O}(k_i, k_i + 3)$  associated with the pair  $(\mathbf{A}(k), \mathbf{C}(k))$  on  $[k_i, k_{i+3}]$ ,  $k_i > k_0$ , has rank equal to the number of states of the system if  $\text{rank}(\mathbf{L}) = 4$ . Fix  $k_i > k_0$  and suppose that the rank of the observability matrix is less than the number of states of the system. Then, there exists a unit vector  $\mathbf{d} \in \mathbb{R}^{7+L+2}$ ,  $\mathbf{d} = [\mathbf{d}_1^T \ \mathbf{d}_2^T \ d_3 \ \mathbf{d}_4^T \ d_5 \ d_6]^T$ , with  $\mathbf{d}_1, \mathbf{d}_2 \in \mathbb{R}^3$ ,  $d_3 \in \mathbb{R}$ ,  $\mathbf{d}_4 \in \mathbb{R}^L$ ,  $d_5, d_6 \in \mathbb{R}$ , such that  $\mathcal{O}(k_i, k_i + 3) \mathbf{d} = \mathbf{0}$  or, equivalently,

$$\begin{cases} \mathbf{C}(k_i) \mathbf{d} = \mathbf{0} \\ \mathbf{C}(k_i + 1) \mathbf{A}(k_i) \mathbf{d} = \mathbf{0} \\ \mathbf{C}(k_i + 2) \mathbf{A}(k_i + 1) \mathbf{A}(k_i) \mathbf{d} = \mathbf{0} \end{cases}. \quad (17)$$

From the first equation of (17), and attending to the structure of  $\mathbf{C}(k_i)$ , one immediately concludes that  $\mathbf{d}_4 = \mathbf{0}$ . Substituting that in the first equation of (17) gives

$$\begin{cases} 2(\mathbf{s}_1 - \mathbf{s}_2)^T \mathbf{d}_1 - \left(\|\mathbf{s}_1\|^2 - \|\mathbf{s}_2\|^2\right) d_3 = 0 \\ 2(\mathbf{s}_1 - \mathbf{s}_3)^T \mathbf{d}_1 - \left(\|\mathbf{s}_1\|^2 - \|\mathbf{s}_3\|^2\right) d_3 = 0 \\ \vdots \\ 2(\mathbf{s}_{L-2} - \mathbf{s}_L)^T \mathbf{d}_1 - \left(\|\mathbf{s}_{L-2}\|^2 - \|\mathbf{s}_L\|^2\right) d_3 = 0 \\ 2(\mathbf{s}_{L-1} - \mathbf{s}_L)^T \mathbf{d}_1 - \left(\|\mathbf{s}_{L-1}\|^2 - \|\mathbf{s}_L\|^2\right) d_3 = 0 \end{cases}. \quad (18)$$

If (16) holds, then the only solution of (18) is  $\mathbf{d}_1 = \mathbf{0}$  and  $d_3 = 0$ . Now, with  $\mathbf{d}_1 = \mathbf{0}$ ,  $d_3 = 0$ , and  $\mathbf{d}_4 = \mathbf{0}$ , one may write, from the second equation of (17), that

$$\begin{cases} (\mathbf{s}_1 - \mathbf{s}_2)^T \mathbf{d}_2 = 0 \\ (\mathbf{s}_1 - \mathbf{s}_3)^T \mathbf{d}_2 = 0 \\ \vdots \\ (\mathbf{s}_{L-2} - \mathbf{s}_L)^T \mathbf{d}_2 = 0 \\ (\mathbf{s}_{L-1} - \mathbf{s}_L)^T \mathbf{d}_2 = 0 \end{cases}. \quad (19)$$

Again, if (16) holds, then the only solution of (19) is  $\mathbf{d}_2 = \mathbf{0}$ . Substituting that in the second equation of (17), together with  $\mathbf{d}_1 = \mathbf{0}$ ,  $d_3 = 0$ , and  $\mathbf{d}_4 = \mathbf{0}$  gives

$$2d_5 + Td_6 = 0. \quad (20)$$

Substituting  $\mathbf{d}_1 = \mathbf{d}_2 = \mathbf{0}$ ,  $d_3 = 0$ , and  $\mathbf{d}_4 = \mathbf{0}$  in the third equation of (17) allows one to write

$$d_5 + Td_6 = 0. \quad (21)$$

The only solution of (20)-(21) is  $d_5 = d_6 = 0$ . But this contradicts the hypothesis of existence of a unit vector  $\mathbf{d}$  such that (17) holds. Hence, the observability matrix must have rank equal to the number of states of the system. As the derivation remains unchanged for any other different  $k_i > k_0$ , the proof is concluded invoking Lemma 1. ■

Finally, it is important to stress that, in the definition of the augmented system (11), the original nonlinear outputs  $r_i(k) = \sqrt{x_3(k+1)} \left\| \mathbf{s}_i - \frac{\mathbf{x}_1(k+1)}{x_3(k+1)} \right\|$ ,  $i = 1, \dots, L$ , were discarded. Furthermore, there is nothing in (11) imposing the nonlinear constraints (8). While it is true that these restrictions could be easily imposed including artificial outputs, e.g.,  $x_{4+L}(k) - \mathbf{x}_1(k) \cdot \mathbf{x}_2(k) / x_3(k) = 0$ , this form was preferred as it allows one to apply Lemma 1. However, care must be taken when extrapolating conclusions from the observability of (11) to the observability of (5). The following theorem addresses this issue and provides the means for design of a state observer or filter for (5), as it will be seen shortly after.

*Theorem 2:* Suppose that (16) holds. Then:

- i) the nonlinear system (5) is observable on any interval  $[k_i, k_{i+3}]$ ,  $k_i = 0, 1, 2, \dots$ , in the sense that the initial state  $\mathbf{x}(k_i)$  is uniquely determined by the input  $\{\mathbf{u}(k) : k = k_i, k_{i+1}, k_{i+2}\}$  and the output  $\{r_1(k), \dots, r_L(k) : k = k_i, k_{i+1}, k_{i+2}\}$ ; and

ii) the initial condition of the augmented nonlinear system (11) corresponds to that of (5), i.e., the relations

$$\begin{cases} \mathbf{x}_1(k_i) = v_s^2(t_{k_i}) \mathbf{p}(t_{k_i}) \\ \mathbf{x}_2(k_i) = v_s^2(t_{k_i}) \mathbf{v}_c(t_{k_i}) \\ x_3(k_i) = v_s^2(t_{k_i}) \\ x_4(k_i) = v_s(t_{k_i}) \|\mathbf{s}_1 - \mathbf{p}(t_{k_i})\| \\ \vdots \\ x_{3+L}(k_i) = v_s(t_{k_i}) \|\mathbf{s}_L - \mathbf{p}(t_{k_i})\| \\ x_{4+L}(k_i) = v_s^2(t_{k_i}) \mathbf{p}(t_{k_i}) \cdot \mathbf{v}_c(t_{k_i}) \\ x_{5+L}(k_i) = v_s^2(t_{k_i}) = \|\mathbf{v}_c(t_{k_i})\|^2 \end{cases}$$

are verified.

*Proof:* Let

$$\mathbf{x}(k_i) := \begin{bmatrix} \mathbf{x}_1(k_i) \\ \mathbf{x}_2(k_i) \\ x_3(k_i) \\ x_4(k_i) \\ \vdots \\ x_{3+L}(k_i) \\ x_{4+L}(k_i) \\ x_{5+L}(k_i) \end{bmatrix} \in \mathbb{R}^{3+3+1+L+2}$$

be the initial condition of (11) and let  $\mathbf{p}(t_{k_i})$ ,  $\mathbf{v}_c(t_{k_i})$ , and  $v_s(t_{k_i})$  be the initial condition of (5). From the first  $L$  outputs of (11) it must be

$$x_{3+j}(k_i) = v_s(t_{k_i}) \|\mathbf{s}_j - \mathbf{p}(t_{k_i})\| = r_j(k_i), \quad (22)$$

$j = 1, \dots, L$ . Considering the differences of squares of the outputs of the nonlinear system (5) for  $k = k_i$  as a function of its initial state yields

$$r_l^2(k_i) - r_m^2(k_i) = \left( \|\mathbf{s}_l\|^2 - \|\mathbf{s}_m\|^2 \right) v_s^2(t_{k_i}) - 2(\mathbf{s}_l - \mathbf{s}_m) \cdot v_s^2(t_{k_i}) \mathbf{p}(t_{k_i}) \quad (23)$$

for all  $l, m \in \{1, \dots, L\}$ ,  $l \neq m$ . On the other hand, evaluating the outputs of (11)  $y_{L+1}(k)$  to  $y_{L+C_2^L}(k)$  for  $k = k_i$  as a function of  $\mathbf{x}(k_i)$ , and using (22) allows to conclude that

$$r_l^2(k_i) - r_m^2(k_i) = \left( \|\mathbf{s}_l\|^2 - \|\mathbf{s}_m\|^2 \right) x_3(k_i) - 2(\mathbf{s}_l - \mathbf{s}_m) \cdot \mathbf{x}_1(k_i) \quad (24)$$

for all  $l, m \in \{1, \dots, L\}$ ,  $l \neq m$ . Comparing (23) with (24), and considering (16), implies that

$$\begin{cases} \mathbf{x}_1(k_i) = v_s^2(t_{k_i}) \mathbf{p}(t_{k_i}) \\ x_3(k_i) = v_s^2(t_{k_i}) \end{cases}. \quad (25)$$

For  $k = k_i + 1$  it is possible to write the differences of squares of the output of (5), as a function of its initial state, as

$$\begin{aligned} r_l^2(k_i + 1) - r_m^2(k_i + 1) &= \left( \|\mathbf{s}_l\|^2 - \|\mathbf{s}_m\|^2 \right) v_s^2(t_{k_i}) \\ &\quad - 2(\mathbf{s}_l - \mathbf{s}_m) \cdot v_s^2(t_{k_i}) \mathbf{p}(t_{k_i}) \\ &\quad - 2T(\mathbf{s}_l - \mathbf{s}_m) \cdot v_s^2(t_{k_i}) \mathbf{v}_c(t_{k_i}) \\ &\quad - 2(\mathbf{s}_l - \mathbf{s}_m) \cdot \mathbf{u}(k) v_s^2(t_{k_i}) \end{aligned} \quad (26)$$

for all  $l, m \in \{1, \dots, L\}$ ,  $l \neq m$ . From the first  $L$  outputs of (11) for  $k = k_i + 1$  it follows that  $x_{L+j}(k_i + 1) = r_j(k_i + 1)$ .

Now, from the outputs  $y_{L+1}(k)$  to  $y_{L+C_2^L}(k)$ , for  $k = k_i + 1$ , of the nonlinear system (11), one may write

$$\begin{aligned} r_l^2(k_i + 1) - r_m^2(k_i + 1) &= \left( \|\mathbf{s}_l\|^2 - \|\mathbf{s}_m\|^2 \right) x_3(k_i) \\ &\quad - 2(\mathbf{s}_l - \mathbf{s}_m) \cdot \mathbf{x}_1(k_i) \\ &\quad - 2T(\mathbf{s}_l - \mathbf{s}_m) \cdot \mathbf{x}_2(k_i) \\ &\quad - 2(\mathbf{s}_l - \mathbf{s}_m) \cdot \mathbf{u}(k) x_3(k_i) \end{aligned} \quad (27)$$

for all  $l, m \in \{1, \dots, L\}$ ,  $l \neq m$ . Comparing (26) with (27), and using (25), gives

$$\begin{cases} (\mathbf{s}_1 - \mathbf{s}_2) \cdot \left[ \mathbf{x}_2(k_i) - v_s^2(t_{k_i}) \mathbf{v}_c(t_{k_i}) \right] = 0 \\ (\mathbf{s}_1 - \mathbf{s}_3) \cdot \left[ \mathbf{x}_2(k_i) - v_s^2(t_{k_i}) \mathbf{v}_c(t_{k_i}) \right] = 0 \\ \vdots \\ (\mathbf{s}_{L-2} - \mathbf{s}_L) \cdot \left[ \mathbf{x}_2(k_i) - v_s^2(t_{k_i}) \mathbf{v}_c(t_{k_i}) \right] = 0 \\ (\mathbf{s}_{L-1} - \mathbf{s}_L) \cdot \left[ \mathbf{x}_2(k_i) - v_s^2(t_{k_i}) \mathbf{v}_c(t_{k_i}) \right] = 0 \end{cases}. \quad (28)$$

If (16) holds, then the only solution of (28) is

$$\mathbf{x}_2 = v_s^2(t_{k_i}) \mathbf{v}_c(t_{k_i}). \quad (29)$$

Expanding the square of the output of the nonlinear system (5) for  $k = k_i + 1$  and  $k = k_i + 2$  as a function of its initial state yields

$$\begin{aligned} r_j^2(k_i + 1) &= r_j^2(k_i) + [\mathbf{u}(k_i) - 2\mathbf{s}_j] \cdot \mathbf{u}(k_i) v_s^2(t_{k_i}) \\ &\quad + 2\mathbf{u}(k_i) \cdot v_s^2(t_{k_i}) \mathbf{p}(k_i) \\ &\quad + 2T[\mathbf{u}(k_i) - \mathbf{s}_j] \cdot v_s^2(t_{k_i}) \mathbf{v}_c(k_i) \\ &\quad + 2T\mathbf{p}(k_i) \cdot v_s^2(t_{k_i}) \mathbf{v}_c(k_i) + T^2 v_s^2(t_{k_i}) \|\mathbf{v}_c(k_i)\|^2 \end{aligned} \quad (30)$$

and

$$\begin{aligned} r_j^2(k_i + 2) &= r_j^2(k_i) + \|\mathbf{u}(k_i) + \mathbf{u}(k_i + 1)\|^2 v_s^2(t_{k_i}) \\ &\quad - 2\mathbf{s}_j \cdot [\mathbf{u}(k_i) + \mathbf{u}(k_i + 1)] v_s^2(t_{k_i}) \\ &\quad + 2[\mathbf{u}(k_i) + \mathbf{u}(k_i + 1)] \cdot v_s^2(t_{k_i}) \mathbf{p}(k_i) \\ &\quad + 4T[\mathbf{u}(k_i) + \mathbf{u}(k_i + 1) - \mathbf{s}_j] \cdot v_s^2(t_{k_i}) \mathbf{v}_c(k_i) \\ &\quad + 4T v_s^2(t_{k_i}) \mathbf{p}(k_i) \cdot \mathbf{v}_c(k_i) + 4T^2 v_s^2(t_{k_i}) \|\mathbf{v}_c(k_i)\|^2 \end{aligned} \quad (31)$$

for  $j = 1, \dots, L$ . On the other hand, expanding the first  $L$  outputs of the nonlinear system (11) for  $k = k_i + 1$  and  $k = k_i + 2$  allows one to write

$$\begin{aligned} r_j^2(k_i + 1) &= r_j(k_i) x_{3+j}(k_i) \\ &\quad + [\mathbf{u}(k_i) - 2\mathbf{s}_j] \cdot \mathbf{u}(k_i) x_3(k_i) \\ &\quad + 2\mathbf{u}(k_i) \cdot \mathbf{x}_1(k_i) + 2T[\mathbf{u}(k_i) - \mathbf{s}_j] \cdot \mathbf{x}_2(k_i) \\ &\quad + 2T x_{4+L}(k_i) + T^2 x_{5+L}(k_i) \end{aligned} \quad (32)$$

and

$$\begin{aligned} r_j^2(k_i + 2) &= r_j(k_i) x_{3+j}(k_i) \\ &\quad + \|\mathbf{u}(k_i) + \mathbf{u}(k_i + 1)\|^2 x_3(k_i) \\ &\quad - 2\mathbf{s}_j \cdot [\mathbf{u}(k_i) + \mathbf{u}(k_i + 1)] x_3(k_i) \\ &\quad + 2[\mathbf{u}(k_i) + \mathbf{u}(k_i + 1)] \cdot \mathbf{x}_1(k_i) \\ &\quad + 4T[\mathbf{u}(k_i) + \mathbf{u}(k_i + 1) - \mathbf{s}_j] \cdot \mathbf{x}_2(k_i) \\ &\quad + 4T x_{4+L}(k_i) + 4T^2 x_{5+L}(k_i) \end{aligned} \quad (33)$$

for  $j = 1, \dots, L$ . Using (22), (25), and (29), and comparing (30) with (32), gives

$$2 \left[ x_{4+L}(k_i) - v_s^2(t_{k_i}) \mathbf{p}(t_{k_i}) \cdot \mathbf{v}_c(t_{k_i}) \right] + T \left[ x_{5+L}(k_i) - v_s^2(t_{k_i}) \|\mathbf{v}_c(t_{k_i})\|^2 \right] = 0 \quad (34)$$

while comparing (31) with (33) yields

$$\left[ x_{4+L}(k_i) - v_s^2(t_{k_i}) \mathbf{p}(t_{k_i}) \cdot \mathbf{v}_c(t_{k_i}) \right] + T \left[ x_{5+L}(k_i) - v_s^2(t_{k_i}) \|\mathbf{v}_c(t_{k_i})\|^2 \right] = 0. \quad (35)$$

The only solution of (34)-(35) is

$$\begin{cases} x_{4+L}(k_i) = v_s^2(t_{k_i}) \mathbf{p}(t_{k_i}) \cdot \mathbf{v}_c(t_{k_i}) \\ x_{5+L}(k_i) = v_s^2(t_{k_i}) \|\mathbf{v}_c(t_{k_i})\|^2 \end{cases}.$$

This concludes the second part of the theorem, as it has been shown that, in the conditions of the theorem, the initial condition of (5) corresponds to that of (11). Now, notice that, using Theorem 1, the initial condition of (11) is uniquely determined. Hence, it follows due to the correspondence between the two systems, that the initial condition of (5) is also uniquely determined. ■

### C. Estimation solution

1) *Augmented system*: The means to design an observer for the quantities  $v_s^2(t_k)$ ,  $\mathbf{p}(t_k)$ ,  $v_s^2(t_k) \mathbf{v}_c(t_k)$ , and  $v_s^2(t_k)$  are provided by Theorem 2 as it is shown that an observer for (11), which can be regarded as linear for observer design purposes, suffices. A simple Kalman filter can be applied, yielding globally exponentially stable error dynamics if the system is shown to be uniformly completely observable [19]. In the paper, the pair  $(\mathbf{A}(k), \mathbf{C}(k))$  was shown to be observable. The proof of uniform complete observability follows similar steps considering uniform bounds in time. An alternative to the Kalman filter could be the design of a Luenberger observer as detailed in [20, Theorem 29.2], which would allow one to choose the convergence rate.

Notice that, even though the ocean current velocity and the factor that accounts for the unknown sound speed velocity are assumed constant, in nominal terms, by appropriate tuning of the Kalman filter it is possible to successfully track slowly time-varying quantities.

2) *Estimation between range measurements*: An observer (or filter) for the discrete-time system (11), as previously derived, only provides estimates when there are range measurements. However, the relative velocity and attitude measurements are usually available at a much higher rate than the range readings. As such, it is possible to obtain estimates of the scaled position, scaled velocity, and speed to propagation of the acoustic waves, at a higher rate, using open-loop propagation between range measurements, as given by

$$\begin{cases} \hat{\mathbf{x}}_1(t) = \hat{\mathbf{x}}_1(t_k) + (t - t_k) \hat{\mathbf{x}}_2(t_k) \\ \quad + \hat{x}_3(t_k) \int_{t_k}^t \mathbf{R}(\tau) \mathbf{v}_r(\tau) d\tau \\ \hat{\mathbf{x}}_2(t) = \hat{\mathbf{x}}_2(t_k) \\ \hat{x}_3(t) = \hat{x}_3(t_k) \end{cases}$$

for  $t_k < t < t_{k+1}$ .

3) *Estimates of  $\mathbf{p}(t)$ ,  $\mathbf{v}_c(t)$ , and  $v_s(t)$* : Estimates for  $\mathbf{p}(t_k)$ ,  $\mathbf{v}_c(t_k)$ , and  $v_s(t)$  follow from the Kalman filter or the Luenberger observer estimates, under some mild assumptions.

*Assumption 1*: The speed of propagation of the acoustic waves in the medium satisfies

$$V_m \leq v_s(t) \leq V_M,$$

with  $V_m, V_M > 0$ .

*Assumption 2*: The inertial position of the vehicle and the ocean current velocity are norm-bounded.

Considering estimates  $\hat{x}_3(t)$  with globally exponentially stable error dynamics, the estimate of the speed of propagation of the acoustic waves in the medium can be obtained from

$$\hat{v}_s(t) = \begin{cases} V_m, & \hat{x}_3(t) < V_m^2 \\ \sqrt{\hat{x}_3(t)}, & V_m^2 \leq \hat{x}_3(t) \leq V_M^2 \\ V_M, & \hat{x}_3(t) > V_M^2 \end{cases}, \quad (36)$$

whose error also converges exponentially fast to zero for all initial conditions under Assumption 1. Estimates for the position and ocean current velocity then follow from

$$\begin{cases} \hat{\mathbf{p}}(t) = \frac{\hat{\mathbf{x}}_1(t)}{\hat{v}_s^2(t)} \\ \hat{\mathbf{v}}_c(t) = \frac{\hat{\mathbf{x}}_2(t)}{\hat{v}_s^2(t)} \end{cases}, \quad (37)$$

and it is possible to show that, under Assumptions 1 and 2, these also converge exponentially fast to zero for all initial conditions. This is established in the following proposition.

*Proposition 1*: Consider an estimator with globally exponentially stable error dynamics for the augmented system (11). Let

$$\begin{cases} \tilde{\mathbf{p}}(t) := \mathbf{p}(t) - \hat{\mathbf{p}}(t) \\ \tilde{\mathbf{v}}_c(t) := \mathbf{v}_c(t) - \hat{\mathbf{v}}_c(t) \\ \tilde{v}_s(t) := v_s(t) - \hat{v}_s(t) \end{cases}$$

denote the estimation errors of the inertial position, the ocean current velocity, and the speed of propagation scale factor. Then, under Assumptions 1 and 2, the estimation errors  $\tilde{\mathbf{p}}(t)$ ,  $\tilde{\mathbf{v}}_c(t)$ , and  $\tilde{v}_s(t)$  converge exponentially fast to zero for all initial conditions.

*Proof*: Let

$$\tilde{\mathbf{x}}(t) = \begin{bmatrix} \tilde{\mathbf{x}}_1(t) \\ \tilde{\mathbf{x}}_2(t) \\ \tilde{x}_3(t) \\ \tilde{x}_4(t) \\ \vdots \\ \tilde{x}_{5+L}(t) \end{bmatrix}$$

denote the estimation error of the estimator with globally exponentially stable error dynamics for the augmented system (11), which means that there exist positive constants  $\alpha$  and  $\lambda$  such that

$$\|\tilde{\mathbf{x}}(t)\| \leq \alpha \|\tilde{\mathbf{x}}(t_0)\| e^{-\lambda(t-t_0)} \quad (38)$$

for all  $t \geq t_0$ . Using simple norm inequalities, it follows from (38) that

$$\|\tilde{\mathbf{x}}_1(t)\| \leq \alpha \|\tilde{\mathbf{x}}(t_0)\| e^{-\lambda(t-t_0)}, \quad (39)$$

$$\|\tilde{\mathbf{x}}_2(t)\| \leq \alpha \|\tilde{\mathbf{x}}(t_0)\| e^{-\lambda(t-t_0)},$$

and

$$|\tilde{x}_3(t)| \leq \alpha \|\tilde{\mathbf{x}}(t_0)\| e^{-\lambda(t-t_0)} \quad (40)$$



for all  $t \geq t_0$ . Next, it is shown that  $\tilde{v}_s(t)$  converges exponentially fast to zero by considering separately the three different cases of (36). Suppose that  $\hat{x}_3(t) < V_m^2$ , which implies, from (36), that  $\hat{v}_s(t) = V_m$ . In that case, one has

$$\begin{aligned}\tilde{x}_3(t) &> x_3(t) - V_m^2 \\ &= v_s^2(t) - V_m^2 \\ &= [v_s(t) + V_m][v_s(t) - V_m] \\ &\geq 2V_m\tilde{v}_s(t),\end{aligned}\quad (41)$$

where the bounds of  $v_s(t)$  were used. In addition, notice that, in this case,  $\tilde{v}_s(t) = v_s(t) - V_m \geq 0$ . Hence, it follows from (41) that

$$|\tilde{v}_s(t)| \leq \frac{1}{2V_m} |\tilde{x}_3(t)| \quad (42)$$

when  $\hat{x}_3(t) < V_m^2$ . Consider now  $V_m^2 \leq \hat{x}_3(t) \leq V_M^2$ . In that case, one has  $\hat{v}_s(t) = \sqrt{\hat{x}_3(t)}$  and hence

$$\begin{aligned}|\tilde{x}_3(t)| &= |v_s^2(t) - \hat{v}_s^2(t)| \\ &= |v_s(t) + \hat{v}_s(t)| |v_s(t) - \hat{v}_s(t)| \\ &\geq 2V_m |\tilde{v}_s(t)|,\end{aligned}\quad (43)$$

where the bounds on  $v_s(t)$  and  $\hat{v}_s(t)$  were used. Thus, one has from (43) that

$$|\tilde{v}_s(t)| \leq \frac{1}{2V_m} |\tilde{x}_3(t)| \quad (44)$$

when  $V_m^2 \leq \hat{x}_3(t) \leq v_M^2$ . Consider now  $\hat{x}_3(t) > V_M^2 > 0$ . In that case, one may write

$$\begin{aligned}|\tilde{x}_3(t)| &= \left| v_s^2(t) - \left[ \sqrt{\hat{x}_3(t)} \right]^2 \right| \\ &= \left| v_s(t) + \sqrt{\hat{x}_3(t)} \right| \left| v_s(t) - \sqrt{\hat{x}_3(t)} \right| \\ &\geq 2V_m \left| v_s(t) - \sqrt{\hat{x}_3(t)} \right|,\end{aligned}\quad (45)$$

where the bounds on  $v_s(t)$  were yet again used. In this case,  $v_s(t) - \sqrt{\hat{x}_3(t)} < 0$  and hence it follows from (45) that

$$|\tilde{x}_3(t)| \geq 2V_m \left[ -v_s(t) + \sqrt{\hat{x}_3(t)} \right]. \quad (46)$$

Also, in this case, one has

$$\begin{aligned}|\tilde{v}_s(t)| &= |v_s(t) - V_M| \\ &= -v_s(t) + V_M \\ &\leq -v_s(t) + \sqrt{\hat{x}_3(t)}.\end{aligned}\quad (47)$$

From (46) and (47) it follows that

$$|\tilde{v}_s(t)| \leq \frac{1}{2V_m} |\tilde{x}_3(t)| \quad (48)$$

when  $\hat{x}_3(t) > V_M^2$ . But then, it has been shown, in (42), (44), and (48), that

$$|\tilde{v}_s(t)| \leq \frac{1}{2V_m} |\tilde{x}_3(t)| \quad (49)$$

for all  $t \geq t_0$ . Substituting (40) in (49) gives

$$|\tilde{v}_s(t)| \leq \frac{1}{2V_m} \alpha \|\tilde{\mathbf{x}}(t_0)\| e^{-\lambda(t-t_0)}, \quad (50)$$

which concludes the proof for  $\tilde{v}_s(t)$ . Next, it is shown that the position error also converges exponentially fast to zero. By definition,

$$\begin{aligned}\tilde{\mathbf{p}}(t) &= \mathbf{p}(t) - \hat{\mathbf{p}}(t) \\ &= \mathbf{p}(t) - \frac{\hat{\mathbf{x}}_1(t)}{\hat{v}_s^2(t)} \\ &= \mathbf{p}(t) - \frac{\mathbf{x}_1(t)}{\hat{v}_s^2(t)} + \frac{\tilde{\mathbf{x}}_1(t)}{\hat{v}_s^2(t)} \\ &= -\frac{\mathbf{p}(t)}{\hat{v}_s^2(t)} [v_s^2(t) - \hat{v}_s^2(t)] + \frac{\tilde{\mathbf{x}}_1(t)}{\hat{v}_s^2(t)} \\ &= -\frac{\mathbf{p}(t)}{\hat{v}_s^2(t)} [v_s(t) + \hat{v}_s(t)] \tilde{v}_s(t) + \frac{\tilde{\mathbf{x}}_1(t)}{\hat{v}_s^2(t)}\end{aligned}\quad (51)$$

for all  $t \geq t_0$ . By assumption, the inertial position is bounded. Let  $\|\mathbf{p}(t)\| \leq P$  for all  $t \geq t_0$ . Using also the bounds for  $v_s(t)$  and  $\hat{v}_s(t)$ , one concludes from (51) that

$$\|\tilde{\mathbf{p}}(t)\| \leq \frac{2V_M}{V_m^2} P |\tilde{v}_s(t)| + \frac{1}{V_m^2} \|\tilde{\mathbf{x}}_1(t)\|. \quad (52)$$

Substituting (39) and (50) in (52) immediately allows one to conclude that the position error also converges exponentially fast to zero. The proof for the error for the ocean current velocity follows similar steps and therefore it is omitted. ■

*Remark 3:* Notice that, according to (50) and (52), not only the error of the estimates provided by (36)-(37) converges exponentially fast to zero but also the convergence rate remains unaffected and it does not depend on the bounds of  $v_s(t)$  stated in Assumption 1. In fact, these bounds only affect the bound of the initial transients.

#### IV. SIMULATION RESULTS

This section presents numerical simulations in order to exemplify the achievable performance with the proposed solution for long baseline navigation with estimation of the scale factor that accounts for the unknown sound velocity of propagation of the acoustic waves.

The initial position of the vehicle is  $\mathbf{p}(0) = [0 \ 0 \ 10]^T$  m, while the ocean current velocity was set to  $\mathbf{v}_c(t) = [-0.1 \ 0.2 \ 0]^T$  m/s. The trajectory that was described by the vehicle is shown in Fig. 2. The LBL configuration is composed

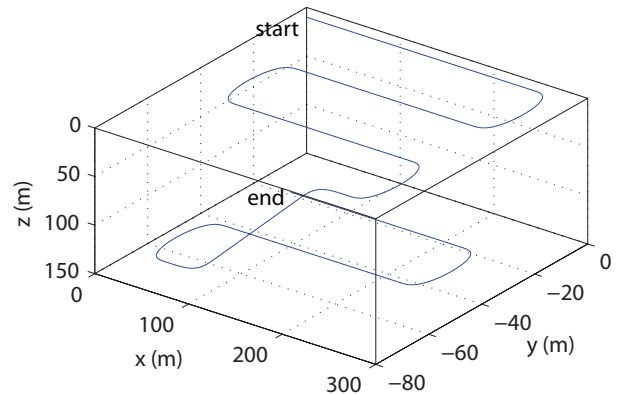


Fig. 2. Trajectory described by the vehicle

of five acoustic transponders and their inertial positions are

$\mathbf{s}_1 = [0 \ 0 \ 1000]^T$  (m),  $\mathbf{s}_2 = [1000 \ 0 \ 500]$  (m),  $\mathbf{s}_3 = [0 \ 750 \ 500]$  (m),  $\mathbf{s}_4 = [0 \ 0 \ 500]$  (m), and  $\mathbf{s}_5 = [1000 \ 1000 \ 500]$  (m), hence satisfying the rank condition (16). The velocity of propagation factor was set to  $v_s(t) = 1.05$ .

Sensor noise was considered for all sensors. In particular, the LBL range measurements and the DVL relative velocity readings were assumed to be corrupted by additive uncorrelated zero-mean white Gaussian noise, with standard deviations of 1 m and 0.01 m/s, respectively. The attitude, provided by the AHRS and parameterized by roll, pitch, and yaw Euler angles, was also assumed to be corrupted by zero-mean, additive white Gaussian noise, with standard deviation of  $0.03^\circ$  for the roll and pitch and  $0.3^\circ$  for the yaw. The sampling period for the range measurements was set to  $T = 1$  s, while the remaining sensors were sampled at 100 Hz. The discrete time input  $\mathbf{u}(k)$ , corresponding to a definite integral, was approximated using the trapezoid rule, while the open-loop solution of the position and ocean current velocity estimates, between range measurements, was computed using the Euler method. In fact, as it also corresponds to a definite integral, it is equivalent to the application of the trapezoid rule.

#### A. Proposed solution

To tune the Kalman filter, the state disturbance covariance matrix was chosen as

$$\text{diag}(10^{-3}\mathbf{I}, 10^{-5}\mathbf{I}, 10^{-5}, 10^{-2}\mathbf{I}, 10^{-2}, 10^{-5})$$

and the output noise covariance matrix was set to

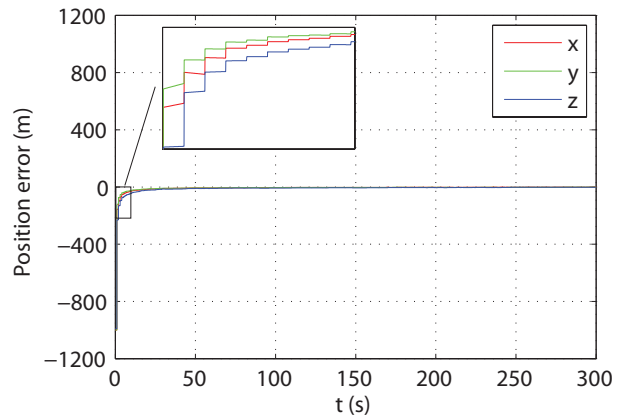
$$\text{diag}(\mathbf{I}, 0.5\mathbf{I}).$$

These values were chosen empirically to adjust the performance of the proposed solution. The initial condition for the position was set with a large initial error,  $\hat{\mathbf{x}}_1(0) = [1000 \ 1000 \ 1000]^T$  (m), while the velocity of propagation factor estimate was set to  $\hat{x}_3(0) = 1$ . The states corresponding to the range measurements were set according to the initial range measurements and the remaining initial state estimates were set to zero.

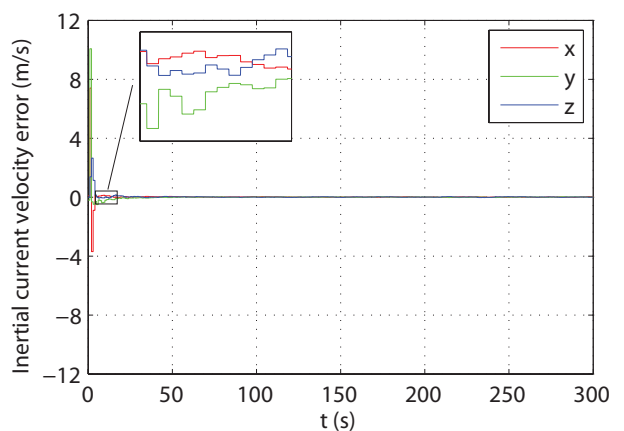
The initial convergence of the position and velocity errors is depicted in Fig. 3, along with details of the discrete-time updates and open-loop propagation between range measurements, which translates into linearly increasing position errors between range measurements (approximately, due to noise). The detailed evolutions of the position and velocity errors are depicted in Figs. 4 and 5, respectively. The most noticeable feature is that the position and velocity errors remain, most of the time, below 1 m and 0.03 m/s, respectively. The evolution of the error of the speed of propagation of the acoustic waves is shown in Fig. 6. The relevant feature here is that the error remains well below 0.5%. For the sake of completeness, the evolution of the range errors is shown in Fig. 7, whereas that of the remaining states is depicted in Fig. 8.

#### B. Performance comparison

The proposed solution was compared with the Extended Kalman Filter (EKF), applied to the original nonlinear system



(a) Position error



(b) Ocean current velocity error

Fig. 3. Initial convergence of the errors

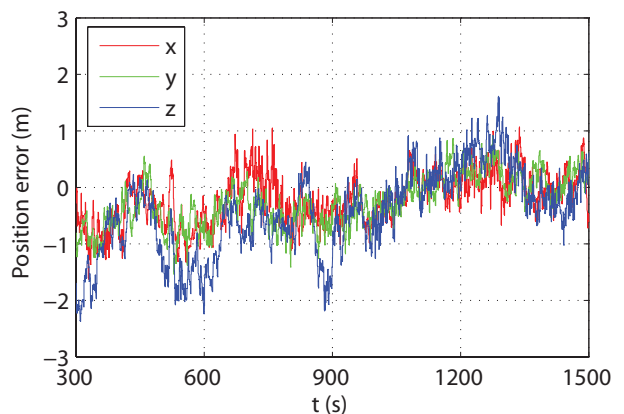


Fig. 4. Steady-state evolution of the position error

(5). The initial estimates were set as in the previous simulation, only now the states that are considered are only the position, the ocean current velocity, and the factor that accounts for the speed of propagation of the waves in the medium. The state disturbance matrix was set to

$$\text{diag}(10^{-2}\mathbf{I}, 5 \times 10^{-5}\mathbf{I}, 10^{-3})$$

and the output noise covariance matrix was set to the identity  $\mathbf{I}$ .

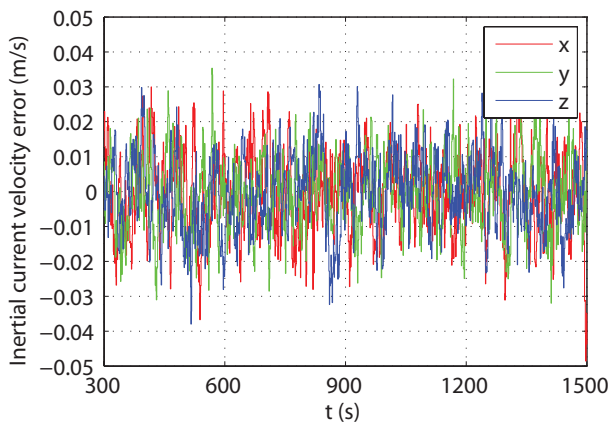


Fig. 5. Steady-state evolution of the ocean current velocity error

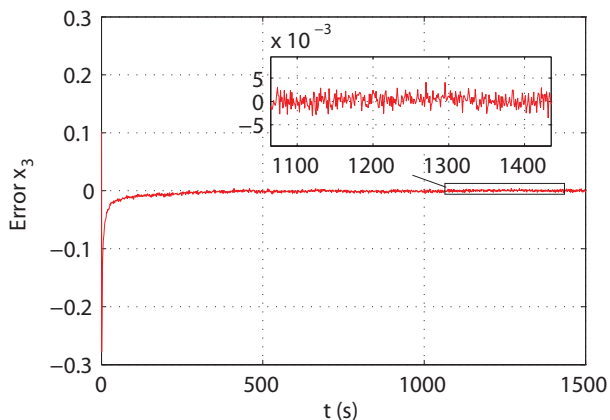


Fig. 6. Evolution of the error of  $x_3(k)$

The initial convergence of the position and velocity errors is depicted in Fig. 9. The initial convergence of the error of the factor that accounts for the speed of propagation of the waves in the medium is shown in Fig. 10. In comparison with the proposed solution, the initial transients exhibited by the EKF are not only much larger but also last longer. The detailed evolutions of the position and velocity errors are depicted in Figs. 11 and 12, respectively. The detailed evolution of the steady-state scale factor error is depicted in Fig. 13. The EKF

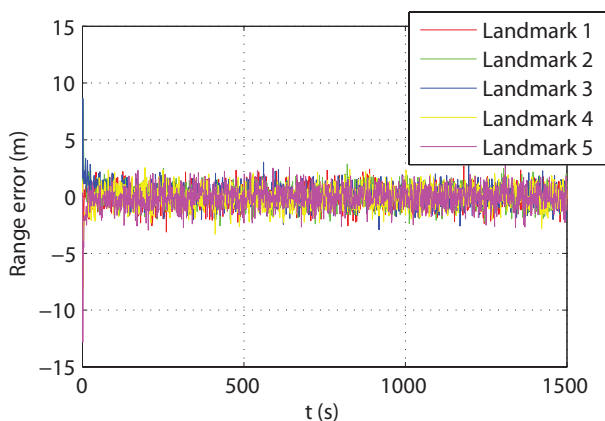


Fig. 7. Evolution of the range errors

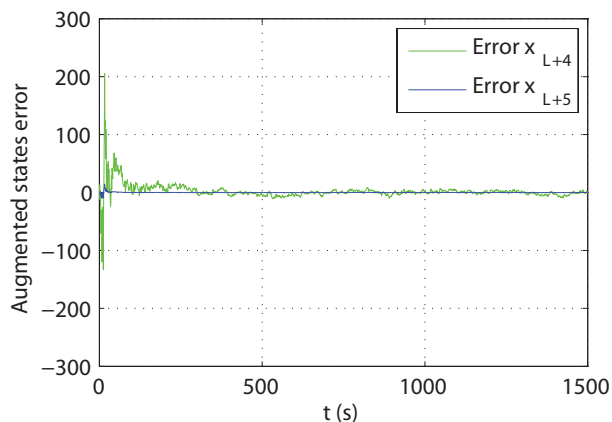
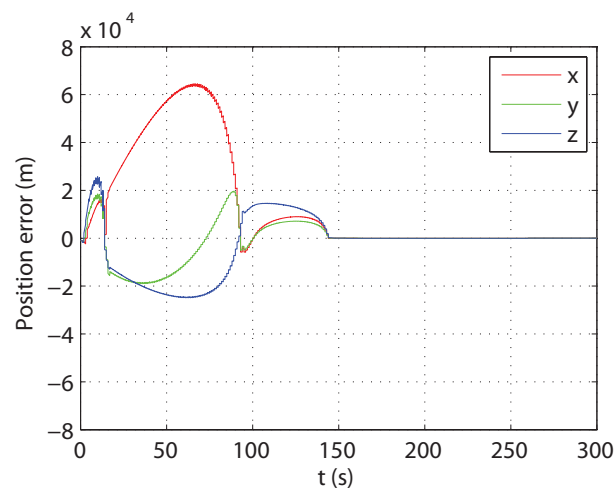
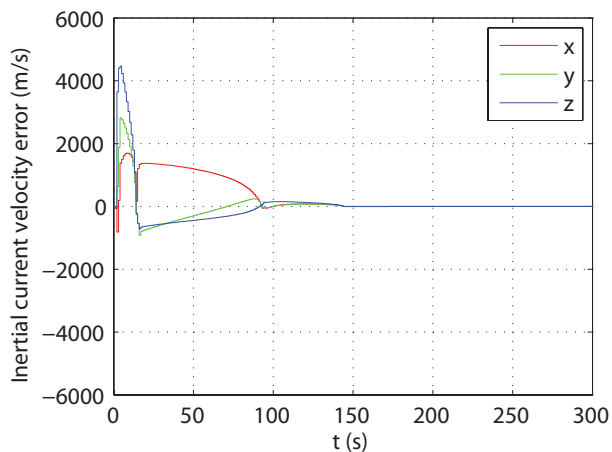


Fig. 8. Evolution of the error of the augmented states  $x_{4+L}(k)$  and  $x_{5+L}(k)$ , in green and blue, respectively



(a) Position error



(b) Ocean current velocity error

Fig. 9. Initial convergence of the EKF errors

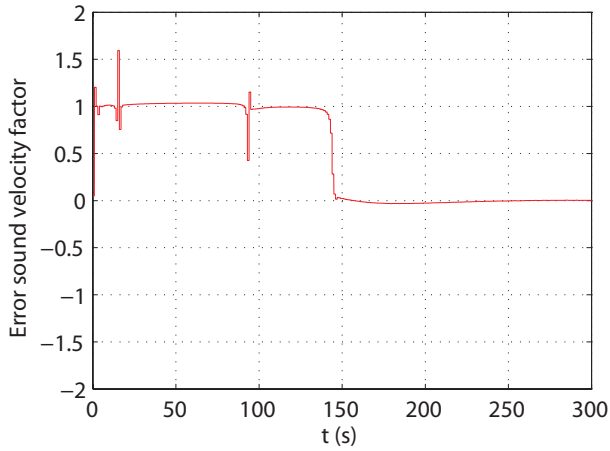
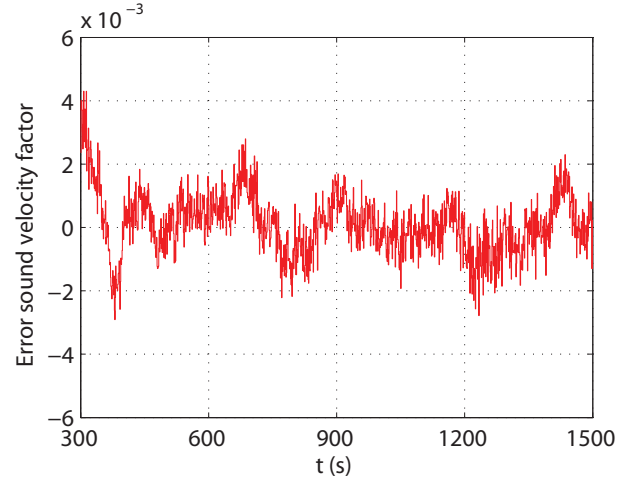
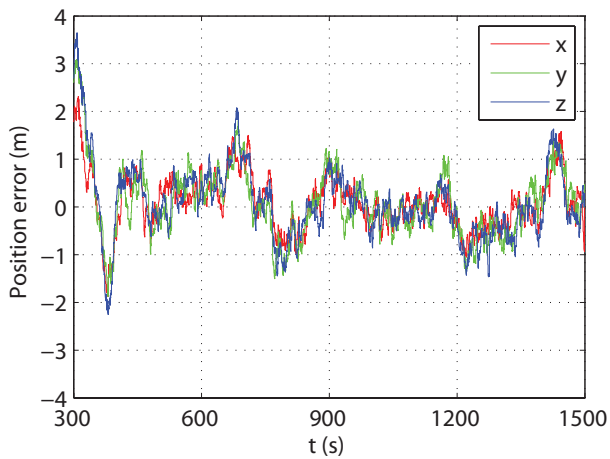
Fig. 10. Evolution of the EKF error of  $v_s(t)$ Fig. 13. Steady-state evolution of the EKF error of  $v_s(t)$ 

Fig. 11. Steady-state evolution of the EKF position error

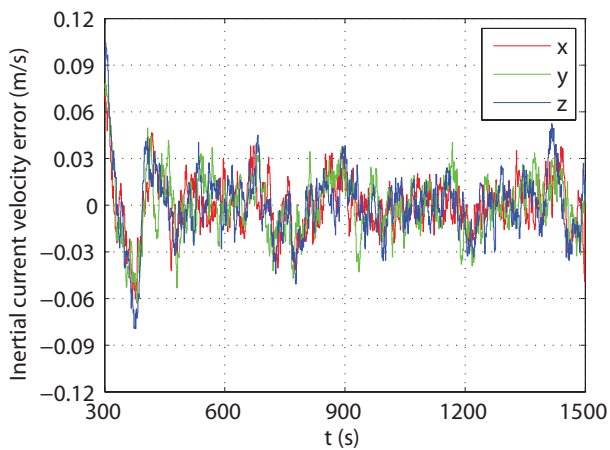


Fig. 12. Steady-state evolution of the EKF ocean current velocity error

TABLE I  
STANDARD DEVIATION OF THE STEADY-STATE ESTIMATION ERROR,  
AVERAGED OVER 1000 RUNS OF THE SIMULATION

| Variable                        | Standard deviation       | EKF standard deviation |
|---------------------------------|--------------------------|------------------------|
| $\tilde{\mathbf{p}}_x$ (m)      | $40.8 \times 10^{-2}$    | $52.5 \times 10^{-2}$  |
| $\tilde{\mathbf{p}}_y$ (m)      | $43.2 \times 10^{-2}$    | $61.5 \times 10^{-2}$  |
| $\tilde{\mathbf{p}}_z$ (m)      | $61.1 \times 10^{-2}$    | $58.3 \times 10^{-2}$  |
| $\tilde{\mathbf{v}}_{cx}$ (m/s) | $11.8 \times 10^{-3}$    | $16.7 \times 10^{-3}$  |
| $\tilde{\mathbf{v}}_{cy}$ (m/s) | $12.0 \times 10^{-3}$    | $18.6 \times 10^{-3}$  |
| $\tilde{\mathbf{v}}_{cz}$ (m/s) | $11.0 \times 10^{-3}$    | $17.5 \times 10^{-3}$  |
| $\tilde{v}_s$                   | not explicitly estimated | $8.46 \times 10^{-4}$  |
| $\tilde{v}_s^2$                 | $1.59 \times 10^{-3}$    | not estimated          |

performs, in steady-state, similarly to the proposed solution. It does not offer, however, global convergence guarantees.

Finally, in order to better evaluate the performance of the proposed solution, the Monte Carlo method was applied, and 1000 simulations were carried out with different, randomly generated noise signals. The standard deviation of the errors were computed for each simulation and averaged over the set of simulations. The results are depicted in Table I. The results with the EKF are also included. As it is possible to observe, both solutions achieve similar performance. Yet, the novel solution proposed in this paper provides global convergence results.

## V. CONCLUSIONS

A common assumption in Long Baseline navigation is that speed of propagation of the acoustic waves in the medium is either known or measured. This paper presents a novel long baseline navigation framework where the factor related to the speed of propagation of the waves is explicitly taken into account and estimated. Considering discrete-time range measurements, an augmented system is proposed that can be regarded, for observability and observer design purposes, as linear. Its observability was analyzed and sufficient conditions were derived. The Kalman filter provides the estimation solution, with globally exponentially stable error dynamics, and DVL and AHRS measurements, obtained at higher rates, are integrated to obtain estimates at high rates. Simulation results evidence fast convergence and good performance, comparable

with that of the Extended Kalman Filter (EKF), which does not offer global convergence guarantees and exhibits longer and larger transients.

#### REFERENCES

- [1] L. Techy, K. Morgansen, and C. Woolsey, "Long-baseline acoustic localization of the Seaglider underwater glider," in *Proceedings of the 2011 American Control Conference*, San Francisco, USA, Jun.-Jul. 2011, pp. 3990–3995.
- [2] L. Whitcomb, D. Yoerger, and H. Singh, "Combined Doppler/LBL Based Navigation of Underwater Vehicles," in *Proceedings of the 11th International Symposium on Unmanned Untethered Submersible Technology*, Durham, New Hampshire, USA, Aug. 1999, pp. 1–7.
- [3] J. Vaganay, J. Bellingham, and J. Leonard, "Comparison of fix computation and filtering for autonomous acoustic navigation," *Int. J. of Systems Science*, vol. 29, no. 10, pp. 1111–1122, Oct. 1998.
- [4] J. Kinsey and L. Whitcomb, "Preliminary field experience with the DVLNAV integrated navigation system for manned and unmanned submersibles," in *Proceedings of the 1st IFAC workshop on guidance and control of underwater vehicles*, Newport, South Wales, UK, Apr. 2003, pp. 83–88.
- [5] M. Larsen, "Synthetic long baseline navigation of underwater vehicles," in *Proceedings of the 2000 MTS/IEEE Oceans*, vol. 3, Providence, RI, USA, Sep. 2000, pp. 2043–2050.
- [6] J. Casey, B. Guimond, and J. Hu, "Underwater Vehicle Positioning Based on Time of Arrival Measurements from a Single Beacon," in *Proceedings of the MTS/IEEE Oceans 2007*, Vancouver, BC, Canada, Sept.–Oct. 2007, pp. 1–8.
- [7] P.-M. Lee, B.-H. Jun, K. Kim, J. Lee, T. Aoki, and T. Hyakudome, "Simulation of an Inertial Acoustic Navigation System With Range Aiding for an Autonomous Underwater Vehicle," *IEEE Journal of Oceanic Engineering*, vol. 32, no. 2, pp. 327–345, Apr. 2007.
- [8] J. Jouffroy and J. Reger, "An algebraic perspective to single-transponder underwater navigation," in *Proceedings of the 2006 IEEE International Conference on Control Applications*, Munich, Germany, Oct. 2006, pp. 1789–1794.
- [9] S. Webster, R. Eustice, H. Singh, and L. Whitcomb, "Preliminary deep water results in single-beacon one-way-travel-time acoustic navigation for underwater vehicles," in *Proceedings of the 2009 IEEE/RSJ International Conference on Intelligent Robots and Systems- IROS 2009*, SaintLouis, MO, USA, Oct. 2009, pp. 2053–2060.
- [10] J. Youngberg, "Method for extending GPS to underwater applications," Jun. 1992.
- [11] H. Thomas, "GIB buoys: an interface between space and depths of the oceans," in *Proceedings of the 1998 Workshop on Autonomous Underwater Vehicles*, Cambridge, MA, USA, Aug. 1998, pp. 181–184.
- [12] A. Alcocer, P. Oliveira, and A. Pascoal, "Study and Implementation of an EKF GIB-based Underwater Positioning System," *Control Engineering Practice*, vol. 15, no. 6, pp. 689–701, Jun. 2007.
- [13] J. Kinsey, R. Eustice, and L. Whitcomb, "A Survey of Underwater Vehicle Navigation: Recent Advances and New Challenges," in *Proceedings of the 7th IFAC Conference on Manoeuvring and Control of Marine Craft*, Lisboa, Portugal, Sep. 2006.
- [14] J. Leonard, A. Bennett, C. Smith, and H. Feder, "Autonomous underwater vehicle navigation," MIT Marine Robotics Laboratory, Tech. Rep. Technical Memorandum 98-1, 1998.
- [15] H.-P. Tan, R. Diamant, W. Seah, and M. Waldmeyer, "A survey of techniques and challenges in underwater localization," *Ocean Engineering*, vol. 38, no. 14-15, pp. 1663–1676, Oct. 2011.
- [16] P. Batista, C. Silvestre, and P. Oliveira, "Sensor-based Long Baseline Navigation: observability analysis and filter design," *Asian Journal of Control*, 2014.
- [17] —, "Single Range Aided Navigation and Source Localization: observability and filter design," *Systems & Control Letters*, vol. 60, no. 8, pp. 665–673, Aug. 2011.
- [18] P. Batista, "GES Long Baseline Navigation with Unknown Sound Velocity and Discrete-time Range Measurements," in *Proceedings of the 52nd IEEE Conference on Decision and Control*, Florence, Italy, Dec. 2013, pp. 6176–6181.
- [19] A. Jazwinski, *Stochastic Processes and Filtering Theory*. Academic Press, Inc., 1970.
- [20] W. Rugh, *Linear system theory*, 2nd ed. Prentice-Hall, Inc., 1995.



**Pedro Batista** (M'10) received the Licenciatura degree in Electrical and Computer Engineering in 2005 and the Ph.D. degree in 2010, both from Instituto Superior Técnico (IST), Lisbon, Portugal. From 2004 to 2006, he was a Monitor with the Department of Mathematics, IST, where he is currently an Invited Assistant Professor with the Department of Electrical and Computer Engineering. His research interests include sensor-based navigation and control of autonomous vehicles. Dr. Batista has received the Diploma de Mérito twice during his graduation and his Ph.D. thesis was awarded the Best Robotics Ph.D. Thesis Award by the Portuguese Society of Robotics.